Research Article

SOCS1/JAK2/STAT3 axis regulates early brain injury induced by subarachnoid hemorrhage via inflammatory responses

https://doi.org/10.4103/1673-5374.313049

Date of submission: July 5, 2020

Date of decision: September 1, 2020

Date of acceptance: January 26, 2021

Date of web publication: April 23, 2021

Yang Wang[1, #], Xiang-Qian Kong[2, 3, #], Fei Wu[1, #], Bin Xu[4], De-Jun Bao[1], Chuan-Dong Cheng[1], Xiang-Ping Wei[1], Yong-Fei Dong[1, *], Chao-Shi Niu[1, 5, *]

Graphical Abstract *Potential role and mechanisms of the SOCS1/JAK2/STAT3 axis regulates early brain injury induced by subarachnoid hemorrhage (SAH) involvement of inflammatory response*

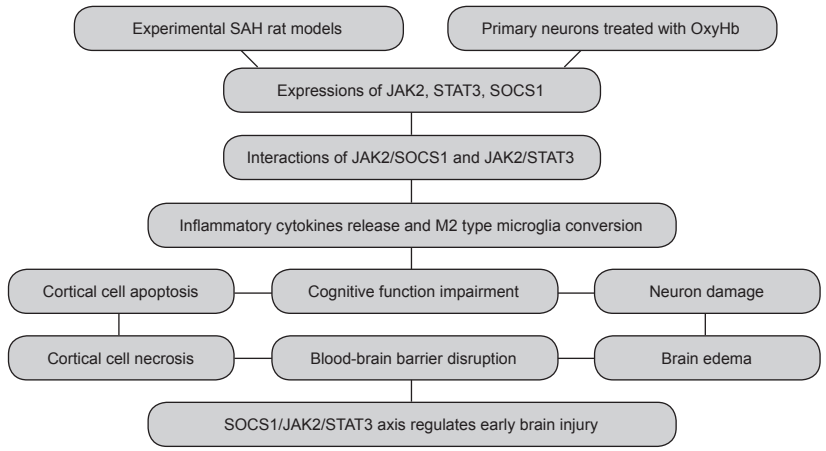

Abstract

The SOCS1/JAK2/STAT3 axis is strongly associated with tumor growth and progression, and participates in cytokine secretion in many diseases. However, the effects of the SOCS1/JAK2/STAT3 axis in experimental subarachnoid hemorrhage remain to be studied. A subarachnoid hemorrhage model was established in rats by infusing autologous blood into the optic chiasm pool. Some rats were first treated with JAK2/STAT3 small interfering RNA (Si-JAK2/Si-STAT3) or overexpression plasmids of JAK2/STAT3. In the brains of subarachnoid hemorrhage model rats, the expression levels of both JAK2 and STAT3 were upregulated and the expression of SOCS1 was downregulated, reaching a peak at 48 hours after injury. Simultaneously, the interactions between JAK2 and SOCS1 were reduced. In contrast, the interactions between JAK2 and STAT3 were markedly enhanced. Si-JAK2 and Si-STAT3 treatment alleviated cortical neuronal cell apoptosis and necrosis, destruction of the blood–brain barrier, brain edema, and cognitive functional impairment after subarachnoid hemorrhage. This was accompanied by decreased phosphorylation of JAK2 and STAT3 protein, decreased total levels of JAK2 and STAT3 protein, and increased SOCS1 protein expression. However, overexpression of JAK2 and STAT3 exerted opposite effects, aggravating subarachnoid hemorrhage-induced early brain injury. Si-JAK2 and Si-STAT3 inhibited M1-type microglial conversion and the release of pro-inflammatory factors (inducible nitric oxide synthase, interleukin-1β, and tumor necrosis factor-α) and increased the release of anti-inflammatory factors (arginase-1, interleukin-10, and interleukin-4). Furthermore, primary neurons stimulated with oxyhemoglobin were used to simulate subarachnoid hemorrhage in vitro, and the JAK2 inhibitor AG490 was used as an intervention. The in vitro results also suggested that neuronal protection is mediated by the inhibition of JAK2 and STAT3 expression. Together, our findings indicate that the SOCS1/JAK2/STAT3 axis contributes to early brain injury after subarachnoid hemorrhage both *in vitro* and *in vivo* by inducing inflammatory responses. This study was approved by the Animal Ethics Committee of Anhui Medical University and the First Affiliated Hospital of University of Science and Technology of China (approval No. LLSC-20180202) on March 1, 2018.

Key Words: brain injury; cytokines; *in vitro* model; *in vivo* model; inflammation; microglia; SOCS1/JAK2/STAT3 axis; subarachnoid hemorrhage

Chinese Library Classification No. R446; R741; R364.5

[1]Department of Neurosurgery, First Affiliated Hospital of University of Science and Technology of China, Division of Life Sciences and Medicine, University of Science and Technology of China, Hefei, Anhui Province, China; [2]Department of Vascular Surgery, Shandong Provincial Hospital Affiliated to Shandong First Medical University, Jinan, Shandong Province, China; [3]Department of Vascular Surgery, Shandong Provincial Hospital, Cheeloo College of Medicine, Shandong University, Jinan, Shandong Province, China; [4]Anhui Medical College, Anhui Provincial Medical Genetics Center, Hefei, Anhui Province, China; [5]Anhui Province Key Laboratory of Brain Function and Brain Disease, Hefei, Anhui Province, China

*__Correspondence to:__ Yong-Fei Dong, MD, dyf.w@163.com; Chao-Shi Niu, PhD, ah_neurosurgery@163.com.

https://orcid.org/0000-0001-8508-567X (Chao-Shi Niu)

#These authors contributed equally to this work.

Funding: *This study was supported by the National Natural Science Foundation of China, No. 81500375 (to XQK); the Fundamental Research Funds for the Central Universities, No. WK9110000112 (to YW); the Anhui Provincial Natural Science Foundation of China, No. 1508085QH184 (to YW); and Shandong Provincial Natural Science Foundation of China, No. ZR2015HQ001 (to XQK).*

How to cite this article: *Wang Y, Kong XQ, Wu F, Xu B, Bao DJ, Cheng CD, Wei XP, Dong YF, Niu CS (2021) SOCS1/JAK2/STAT3 axis regulates early brain injury induced by subarachnoid hemorrhage via inflammatory responses. Neural Regen Res 16(12):2453-2464.*

Introduction

Subarachnoid hemorrhage (SAH) belongs to a very serious type of hemorrhagic cerebrovascular disease, and is typically defined by the sudden filling with blood of the subarachnoid space. This severe cerebrovascular disease often leads to patient death, and makes up approximately 5% of all strokes (Korja and Kaprio, 2016; Macdonald and Schweizer, 2017). Each year, 6 percent of the world's population will have an aneurysm in the brain, and approximately 10 out of every 100,000 people will have an aneurysm rupture for various reasons, thereby inducing SAH (Sturiale et al., 2013). With the general enhancement of health awareness and advances in neuroimaging technology, unruptured intracranial aneurysms can be detected earlier. However, if an intracranial aneurysm located in the subarachnoid space ruptures and evokes SAH, the consequences are undoubtedly fatal (Hall and O'Kane, 2018). The underlying mechanisms of damage associated with SAH remain unclear. Previous studies have demonstrated that there are two main mechanisms of SAH-induced brain injury: the involvement of early brain injury (EBI) and cerebral angiospasm, of which EBI is regarded as the main pathogenic factor (Hasegawa et al., 2017; Vadokas et al., 2019; Chen et al., 2020). The two vital events that promote EBI are neuronal apoptosis and necrosis, and studies have shown that inflammation after SAH can also contribute to EBI (Tong et al., 2020). Thus, the inflammatory response has a lethal effect on the development of SAH.

When SAH occurs, hemoglobin accumulation in the subarachnoid space stimulates endothelial cells to rapidly express a large number of cell adhesion molecules, attracting neutrophils to aggregate. These aggregated cells become trapped in the subarachnoid space, and may participate in vasospasm through enzymatic activity related to oxidative bursts (Ahn et al., 2019). Monocytes accumulate in the injured tissue and become macrophages, and lymphocytes and macrophages release inflammatory cytokines into the cerebrospinal fluid (Schneider et al., 2018). Blood-brain barrier (BBB) injury further promotes the release of inflammatory factors (Liu et al., 2018; Zhang and Cai, 2020). A marked increase in proinflammatory factors, including interleukin (IL)-1, IL-6, and tumor necrosis factor-α (TNF-α), has been reported to be closely linked to unfavorable prognosis in SAH, and IL-1 receptor antagonist treatment can alleviate this situation (Okada and Suzuki, 2017). Experiments have demonstrated that neuroinflammation is related to cognitive dysfunction in other diseases (Rosenblat et al., 2015), and it may therefore be a potential mechanism for such defects in SAH patients.

The Janus kinase/signal transducers and activators of transcription (JAK/STAT) signaling pathway has been extensively studied, and controls gene expression in tumor and immune cells (Pencik et al., 2016). Many experiments have demonstrated that JAK/STAT signal pathway activation promotes tumor growth and progression (Groner and von Manstein, 2017). It has also been reported that both STAT3 and STAT5 can promote the growth and development of breast cancer, and that STAT3 activation inside tumor cells can accelerate tumor cell growth. In addition, suppressing STAT3 expression in breast cancer models leads to reduced tumor cell proliferation and invasiveness (Shi et al., 2015; Qin et al., 2019). Therefore, the JAK/STAT signaling pathway is now being investigated as a potential therapeutic option in breast cancer (Lim et al., 2012). The JAK/STAT pathway also has an important impact on cytokines mediated by inflammatory responses in brain microvascular endothelial cells, and its activation is reportedly associated with astrocyte activation and increased IL-6 levels (Matsumoto et al., 2018). For example, curcumin can alleviate the inflammatory response after cerebral ischemia by inhibiting the JAK2/STAT3 signaling pathway (Wu et al., 2018). Nevertheless, the function of the JAK/STAT signaling pathway in EBI after SAH has not yet been investigated, especially with regard to the classification of microglial activation, inflammatory cytokine release, and other potential mechanisms.

Suppressors of cytokine signaling (SOCS) proteins are a type of cellular protein that can suppress cytokine signal transduction in many cell types. They perform such functions by integrating with subunits of cytokine receptors and tyrosine phosphorylation sites on JAK, thereby disturbing the classic JAK/STAT pathway by accelerating proteasome degradation of sensitized receptors and eliminating stimulation to continue activating the transmission pathway (Morris et al., 2018; Durham et al., 2019). In terms of function, SOCS-1 and SOCS-3 are the two best-studied SOCS genes, and have important roles in regulating inflammation (Qin et al., 2012; Wang et al., 2018). Both SOCS-1 and SOCS-3 are expressed in microglia, but only SOCS-1 can inhibit M1-phenotype production and induce M2-phenotype differentiation (Walker et al., 2015).

Thus, we aimed to investigate the role of the SOCS1/JAK2/STAT3 axis and its underlying mechanisms of brain damage in EBI in a rat model of SAH, and explored the inflammatory response in this process.

Materials and Methods

Experimental animals

In total, 420 male adult clean-grade Sprague-Dawley rats aged 8 weeks (weighing 300–350 g) were supplied by the Laboratory Animal Center of Anhui Medical University, China (production license No. SCXK (Wan) 2017-001; user license No. SYXK (Wan) 2017-006).

All rats were kept separately at a constant temperature (18–26°C) and humidity (40–70%). All animal experiments were approved and supervised by the Animal Ethics Committee of Anhui Medical University and the First Affiliated Hospital of University of Science and Technology of China (approval No. LLSC-20180202) on March 1, 2018. The feeding and use of laboratory animals were performed in strict accordance with the guidelines of the National Institutes of Health (USA).

SAH rat model

As in our previous study (Wang et al., 2019), we established a SAH rat model via the stereotactic injection of autologous blood into the optic chiasm cistern. First, the animals were fixed in a stereotaxic apparatus (Anhui Zhenghua Biological Equipment Co., Ltd., Hefei, China) after being anesthetized by intraperitoneal injection of 4% chloral hydrate (1 mL/100 g; Sigma-Aldrich, St. Louis, MO, USA). After the skull was drilled, a side needle with a round tip and a side hole located on the bottom was inserted stereoscopically into the anterior skull base. The entry point was located at the anterior midline of the sagittal point, 7.5 mm anterior to the anterior fontanelle. The puncture direction was at a 45° angle to the coronal plane. The syringe was lowered until the tip reached the bottom of the skull, and then retracted by 0.5 mm. A syringe pump was used to slowly inject 300 µL fresh, non-heparinized autologous blood into the prechiasmatic cistern over 20 seconds. In the Sham group, 300 µL physiological saline was injected in the same way. After 45 minutes of recovery, all rats were returned to the cage. At different points in time after SAH, the animals were deeply anesthetized and 60 mL ice-cold phosphate-buffered saline was infused into the heart. Brain tissue covered by blood clots was then selected for analysis.

Transfection of plasmids and small interfering RNA *in vivo*

Three different types of plasmids (Genescript, Nanjing, China) were intracerebroventricularly injected: one overexpressed rat JAK2 (Over-JAK2; Gene ID number: 3717), one overexpressed rat STAT3 (Over-STAT3; Gene ID number: 6774), and the remaining empty-vector plasmid (Vector) was used as the negative control. All plasmids were stored

at –80°C, and were diluted at 0.5 mg/mL in the transfection solution before being injected into the lateral ventricle. Three different types of small interfering RNA (siRNA; Genescript, Nanjing, China) were also used: two of them were specific to rat JAK2 and STAT3 mRNA, which silenced their transcription. Scramble siRNA (si-NC) was used as the negative control. According to the manufacturer's instructions (Engreen, Shanghai, China), 500 pmol si-JAK2 and si-STAT3 and 500 pmol scramble siRNA were dissolved in 5 µL RNase-free water. Next, 10 µL Entranster (Genescript, Nanjing, China) was added to 5 µL scrambled siRNA, JAK2 siRNA, or STAT3 siRNA solution *in vivo*, and the solution was mixed for 15 minutes. Finally, an intraventricular injection of the Entranster transfection reagent-*in vivo*–siRNA mixture was performed 48 hours before the SAH procedure.

Primary neuron culture

According to a previous study (Li et al., 2018b), primary neurons were isolated and cultured from rat embryos on day 18 (Zhaoyan New Drug Research Center, Suzhou, Jiangsu, China). Rat embryonic cerebral tissue was first placed in precooled phosphate-buffered saline (approximately 4°C), and the meninges and capillaries located on the surface of the hemisphere were separated on ice and wiped to maintain cellular activity. Brain tissue was percussed and digested for 5 minutes after adding 0.25% trypsin. The mixed liquid was then centrifuged at 16,000 × *g* for 5 minutes. Next, the deposit was mixed with Neurobasal Medium containing 2% B27, 0.5 mM GlutaMAX^{TM}-1, 50 U/mL penicillin, and 50 U/mL streptomycin. Finally, neurons were inoculated in 6- and 12-well plates pre-coated with poly-D-lysine (Sigma-Aldrich) containing fresh Neurobasal Medium at a density of 20,000 cells/cm^2. The culture was kept in a 5% CO_2 and 37°C atmospheric incubator for 1 week, and half of the medium was replaced every other day. Simultaneously, the neurons were stimulated with oxygenated hemoglobin (oxyHb) to create an *in vitro* model of SAH, with AG490 (a kind of JAK inhibitor; Sigma-Aldrich) used as the intervention. Briefly, oxyHb was dissolved in phosphate-buffered saline (10 µM) and added to culture medium when the neuron network structure had just been formed. Next, we continued to incubate the neurons under the same environment for 48 hours after oxyHb stimulation. Finally, the medium was siphoned from the plates, and primary neurons were scratched or fixed with 4% paraformaldehyde, after which all relevant experiments were performed.

Experimental design and intervention

Experiment 1 was designed to confirm the involvement of the SOCS1/JAK2/STAT3 axis in EBI following SAH (**Figure 1A**). Specifically, 42 rats were randomly assigned to seven groups (n = 6): Sham; 6-, 12-, 24-, 48-, and 72-hour; and 1-week SAH groups. Subtemporal brain tissue below the blood clot was obtained for our study. Brain tissue was obtained from SAH rats at different time points for western blot, immunofluorescence, and immunoprecipitation assays.

Experiment 2 was designed to examine the brain injury mechanisms of the SOCS1/JAK2/STAT3 axis in EBI induced by SAH (**Figure 1B**). Rats received an intracerebroventricular injection of JAK2 or STAT3 siRNA (Si-JAK2, Si-STAT3), or overexpression plasmids of JAK2 or STAT3 (Over-JAK2, Over-STAT3), 2 days before the SAH procedure. In total, 192 rats were randomly assigned to eight groups (n = 24): Sham, SAH, Si-NC, Si-JAK2, Si-STAT3, Vector, Over-JAK2, and Over-STAT3 groups. The temporal lobes of 12 rats per group were sectioned and used for immunofluorescence staining, Fluoro-Jade B staining, and terminal deoxynucleotidyl transferase-mediated dUTP nick end labeling (TUNEL) staining. The brains of the remaining 12 rats in each group were used for western blot assay and brain edema evaluation.

Experiment 3 was designed to assess the effects of the SOCS1/JAK2/STAT3 axis on cognitive and motor function (**Figure 1C**). We randomly divided 96 adult male rats into eight groups (n = 12): Sham, SAH, Si-NC, Si-JAK2, Si-STAT3, Vector, Over-JAK2, and Over-STAT3 groups. The adhesive-removal, rotarod, and Morris water maze tests were conducted in the different groups.

Experiment 4 was designed to explore the roles of the SOCS1/JAK2/STAT3 axis *in vitro* (**Figure 1D**). OxyHb was used to treat primary cultured neurons, and AG490 was used as the intervention. Cells were divided into four groups: Control, OxyHb, Vehicle, and AG490 (50 µM) groups.

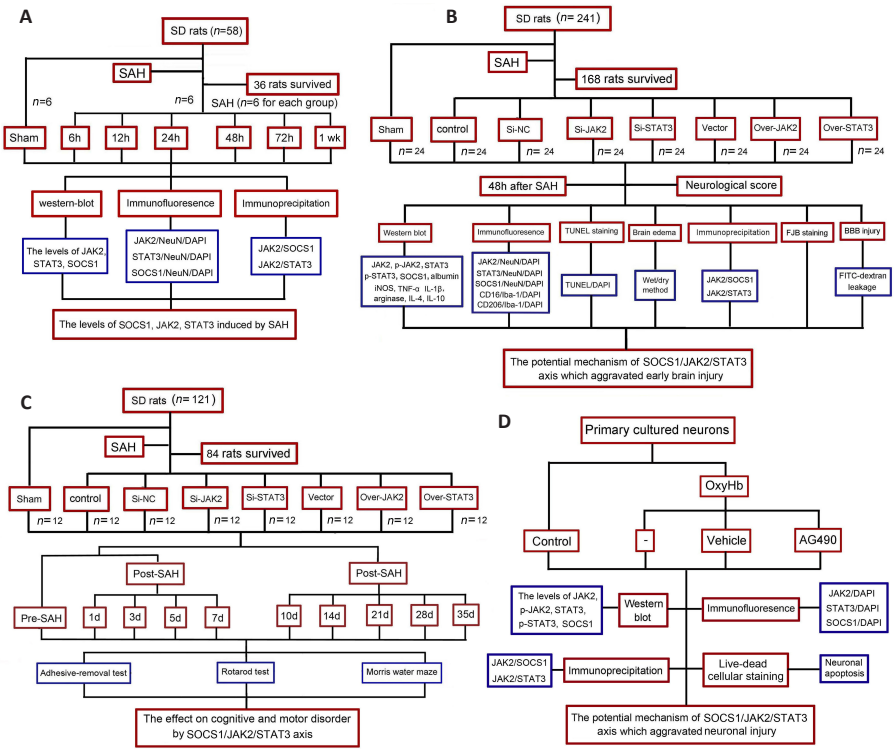

Figure 1 | **Experimental design.**
(A, D) Experiments 1 and 4 were designed to determine the involvement of the SOCS1/JAK2/STAT3 axis in EBI under *in vitro* and *in vivo* SAH conditions. (B, C) Experiments 2 and 3 were designed to determine the involvement of neuroprotection through the SOCS1/JAK2/STAT3 axis via suppression of the inflammatory response. AG490: Tyrphostin AG 490; BBB: blood-brain barrier; DAPI: 4′,6-diamidino-2-phenylindole; FJB: Fluoro-Jade B; EBI: early brain injury; IL: interleukin; JAK2: Janus kinase 2; oxyHb: oxyhemoglobin; SAH: subarachnoid hemorrhage; SD: Sprague-Dawley; Si-JAK2: JAK2 small interfering RNA; Si-NC: negative control small interfering RNA; Si-STAT3: STAT3 small interfering RNA; SOCS1: suppressors of cytokine signaling 1; STAT3: signal transducer and activator of transcription 3; TNF: tumor necrosis factor; TUNEL: terminal deoxynucleotidyl transferase-mediated dUTP nick end labeling.

Western blot assay

Western blot assays were conducted at 48 hours after SAH as previously described (Wang et al., 2019). Brain samples and neurons were lysed using western blot lysis buffer supplemented with phenylmethylsulfonyl fluoride. Protein concentrations were estimated using the bicinchoninic acid method (Wang et al., 2015). Protein samples (20 μg/lane) and molecular weight markers (8 μL/lane) were loaded on a 10% sodium dodecyl-polyacrylamide electrophoresis gel, separated, and electrophoretically transferred to nitrocellulose membranes. The membranes were sealed with 5% skim milk for 1 hour at room temperature and incubated with anti-albumin (1:2000, Cat# ab207327; Abcam), -p-JAK2 (1:1000, Cat# ab195055; Abcam), -JAK2 (1:1000, Cat# ab108596; Abcam), -p-STAT3 (1:1000, ab76315; Abcam), -STAT3 (1:1000, Cat# ab119352; Abcam), and -SOCS1 (1:1500, Cat# ab62584; Abcam) antibodies overnight at 4°C. β-Tubulin was used as the loading control. Membranes were then incubated with horseradish peroxidase-conjugated anti-mouse IgG (1:3000, Cat# 7076S; Cell Signaling Technology, Boston, MA, USA) and horseradish peroxidase-conjugated anti-rabbit IgG (1:3000, Cat# 7074s; Cell Signaling Technology) at room temperature for 1 hour. After developing solution was added to the membranes, the protein bands were detected using a luminescent image analyzer (Clinx ChemiScope5300, Clinx Science Instruments, Shanghai, China). Protein levels were analyzed using ImageJ software (National Institutes of Health, Bethesda, MD, USA) and normalized to the relative density of the Sham or Control group. The ratio of phosphoprotein to total protein was used for evaluating phosphorylation levels.

Immunofluorescence assay

Immunofluorescence staining was conducted on paraffin-embedded sections at 48 hours after SAH (Wang et al., 2017). Dewaxed sections and neurons were incubated at 4°C overnight with the following antibodies: rabbit anti-JAK2 monoclonal (1:300, Cat# ab108596; Abcam), rabbit anti-NeuN monoclonal (1:300, Cat# ab177487; Abcam), rabbit anti-CD16 monoclonal (1:300, Cat# ab246222; Abcam), mouse anti-STAT3 monoclonal (1:100, Cat# ab119352; Abcam), mouse anti-NeuN monoclonal (1:300, Cat# ab104224; Abcam), mouse anti-SOCS1 monoclonal (1:100, Cat# sc-518028; Santa Cruz Biotechnology, Santa Cruz, CA, USA), and mouse anti-Iba1 monoclonal (1:100, Cat# sc-32725; Santa Cruz Biotechnology). The following day, they were washed three times and incubated with Alexa Fluor 488-conjugated donkey anti-rabbit IgG (H+L) (1:300, Cat# A32790; Invitrogen), Alexa Fluor 555-conjugated donkey anti-rabbit IgG (H+L) (1:300, Cat# A32794; Invitrogen), Alexa Fluor 488-conjugated goat anti-mouse IgG (H+L) (1:300, Cat# A-11001; Invitrogen), and Alexa Fluor 555-conjugated goat anti-mouse IgG (H+L) (1:300, Cat# A-21424; Invitrogen) at 37°C for 1 hour. Next, sections were added to 4,6-diamino-2-phenylindole (SouthernBiotech, Birmingham, AL, USA) for coverslipping. Brain regions were then observed under a fluorescence microscope (BX50/BX-FLA/DP70; Olympus, Tokyo, Japan), and ImageJ software was used to quantify fluorescence intensity. At least one section was stained per rat, and at least three micrographs were taken per section.

Immunoprecipitation assay

Immunoprecipitation detection was conducted at 48 hours after SAH using experimental procedures based on those of a previous study (Li et al., 2018a). First, radioimmunoprecipitation assay buffer was added to lyse the brain samples and neurons. The lysate was incubated with rabbit anti-JAK2 monoclonal antibody (1:100, Cat# ab108596; Abcam) or anti-rabbit IgG (1:100, Cat# ab172730; Abcam) overnight at 4°C with orbital shaking. Protein A + G Sepharose beads (1:250, Cat# ab193262; Abcam) were then added to every immunocomplex. Simultaneously, the pyrolysis mixture was incubated for 4 hours at 4°C under orbital shaking. The immunoblotting method was then used to isolate and detect proteins.

BBB permeability

BBB permeability at 48 hours after SAH was evaluated by the amount of albumin exudation from cerebral microvessels (Yuan et al., 2019). Under normal physiological conditions, brain concentrations of albumin are low because of the integrity of the BBB. However, albumin content in the brain is reported to increase when the BBB is damaged (Yuan et al., 2019). Thus, albumin levels in the brain tissue of each group were detected by western blot assay. In addition, as described in a previous study (Yuan et al., 2019), 0.2 mL 2% fluorescein isothiocyanate-dextran (FITC-dextran) (100 μg/mL; Sigma-Aldrich) was injected into each rat via the femoral vein to examine low molecular-weight molecular leakage. Systemic intracardiac perfusion was performed 2 hours later with saline supplemented with 1 USP U/mL heparin (Sigma-Aldrich) to flush the intravascular FITC-dextran. The perfused brain was then collected, ground, and centrifuged. Supernatant fluorescence represented FITC-dextran content and was measured using an EnSpire Manager Multimode Plate Reader (PerkinElmer, Waltham, MA, USA).

Brain edema assay

The wet and dry weight method was used to assess the cerebral edema index at 48 hours after SAH (Wang et al., 2019). Fresh brain tissue was collected and promptly weighed to record the wet weight. The sample was then dried at 100°C for 72 hours, and then weighed as the dry weight. The cerebral edema index (%) was calculated as [(wet weight – dry weight)/wet weight] × 100.

TUNEL staining

TUNEL staining was used to evaluate cortical cell apoptosis using an In Situ Cell Death Detection Kit (Sigma-Aldrich) at 48 hours after SAH. Briefly, rat brain sections were incubated with 0.1% Triton X-100 for 8 minutes, washed three times, and then reacted with the TUNEL reaction mixture at 37°C for 1 hour. After washing the brain sections with phosphate-buffered saline with Tween-20, 4,6-diamino-2-phenylindole was added to cover the sections. Finally, the sections were observed under a fluorescent microscope. To estimate the degree of cortical cell apoptosis, the ratio of TUNEL-positive cells (red fluorescence) was recorded as the apoptotic index for each section.

Fluoro-Jade B staining

Fluoro-Jade B is a highly sensitive and specific fluorescent dye that can be used to indicate neuronal degradation (Armstead et al., 2019), and it was detected at 48 hours after SAH. Briefly, brain sections were dewaxed before being immersed in 0.06% $KMnO_4$ solution for 15 minutes in the dark at room temperature. Sections were then incubated with Fluoro-Jade B working solution (Sigma-Aldrich) (with 0.1% acetic acid solvent) for 1 hour, air dried at room temperature, and sealed with neutral balsam mounting medium. Finally, six microscope fields per tissue section, in three sections per rat, were observed under a fluorescence microscope. Pictures were taken in parallel to count the Fluoro-Jade B-positive cells.

Adhesive-removal test

This test was used to assess SAH-induced deficiencies in sensory and motor coordination abilities (Li et al., 2019). Each rat was placed in a glass box and a circular sticker was stuck to the palm of each forepaw. The time it took for the rat to remove all stickers was recorded. The rats were trained daily for 3 days prior to the SAH procedure. Testing was performed at 1 day before and 1, 3, 5, 7, 10, 14, 21, 28, and 35 days after the SAH procedure.

Rotarod test

This test was adopted to evaluate the motor abilities of rats using a rotating cylinder provided by Anhui Zhenghua Biological Equipment Co., Ltd. Rats were placed on the horizontal axis, set at a stationary rate from 4 to 30 r/min, for 1 minute. When rats fell to the ground or gripped the device for two revolutions, the test was immediately terminated and the time the animal remained on the axis was recorded. Similar to the adhesive-removal test, experimental rats were trained for 3 days prior to the SAH procedure. Testing was performed at 1 day before and 1, 3, 5, 7, 10, 14, 21, 28, and 35 days after the SAH procedure.

Morris water maze

The Morris water maze test was conducted as described previously (Yuan et al., 2019). The Morris water maze device consisted of a circular pool with a diameter of 2 m and a height of 0.75 m. A mixture of water and melanin filled the circular pool at 25°C, with 0.4 m depth. Four equidistant points were randomly determined as North, South, East, and West to constitute four equivalent quadrants (Northwest, Northeast, Southeast, and Southwest). We place a circular platform of a diameter of 12 cm in constant position, 2 cm below the surface of the water. A vidicon installed on the ceiling above the swimming pool was used to track the trajectories of the experimental animals. Rats in the experimental groups received 4 consecutive days of training before the formal testing. Each trial time limit was 60 seconds, and the inter-trial interval time was 5 minutes. If a rat reached the platform within 60 seconds, it was allowed to rest on the platform for 15 seconds. If a rat failed to reach the platform within 60 seconds, it was guided to the platform. Morris water maze tests were performed at 1 day before and 1, 3, 5, 7, 10, 14, 21, 28, and 35 days after the SAH procedure.

Live/dead cell staining *in vitro*

Neuronal apoptosis was examined by live/dead cell staining at 48 hours after oxyHb intervention. A calcein-AM/propidium iodide double-staining kit (Thermo Fisher Scientific, Shanghai, China) was used to detect apoptosis in cultured neurons according to the manufacturer's instructions. First, culture medium was removed and the live neurons were washed three times. Next, the pre-configured working reagent was mixed with calcein-AM and propidium iodide, added to the neurons, and incubated for 30 minutes at room temperature. The apoptosis rate was analyzed by counting cells under a fluorescence microscope.

Statistical analysis

GraphPad Prism 7.0 software (GraphPad, San Diego, CA, USA) was used for all data processing and analyses. Data are shown as the mean ± SEM. One-way or two-way ANOVA was used for multiple comparisons followed by Scheffé F *post hoc* test . $P < 0.05$ was considered significant.

Results

The SOCS1/JAK2/STAT3 axis is activated following SAH

To detect changes in JAK2, STAT3, and SOCS1 expression after SAH, we performed western blot assay, immunoprecipitation, and immunofluorescent staining. Western blot results demonstrated that the expression levels of JAK2 and STAT3 were markedly higher after SAH; conversely, SOCS1 expression was lower compared with the Sham group. Expression of the three proteins attained a peak at 48 hours and then gradually recovered within 1 week ($P < 0.01$ or $P < 0.05$; **Figure 2A–D**). Compared with the Sham group, the interaction between JAK2 and SOCS1 was significantly lower and the interaction between JAK2 and STAT3 was significantly higher after SAH at 48 hours ($P < 0.01$ or $P < 0.05$; **Figure 2E–H**). Furthermore, immunofluorescence also showed that the immunopositivity of JAK2 and STAT3 was higher, while the immunopositivity of SOCS1 was lower, at each time point after SAH compared with the Sham group ($P < 0.01$ or $P < 0.05$; **Figure 3A–F**). These results indicate that the SOCS1/JAK2/STAT3 axis may participate in pathological processes during EBI, and is apparently activated following SAH. Furthermore, 48 hours after SAH might be the most appropriate time point for interventions in Experiments 2 and 3. Therefore, 48 hours was regarded as the optimal intervention point for further studies.

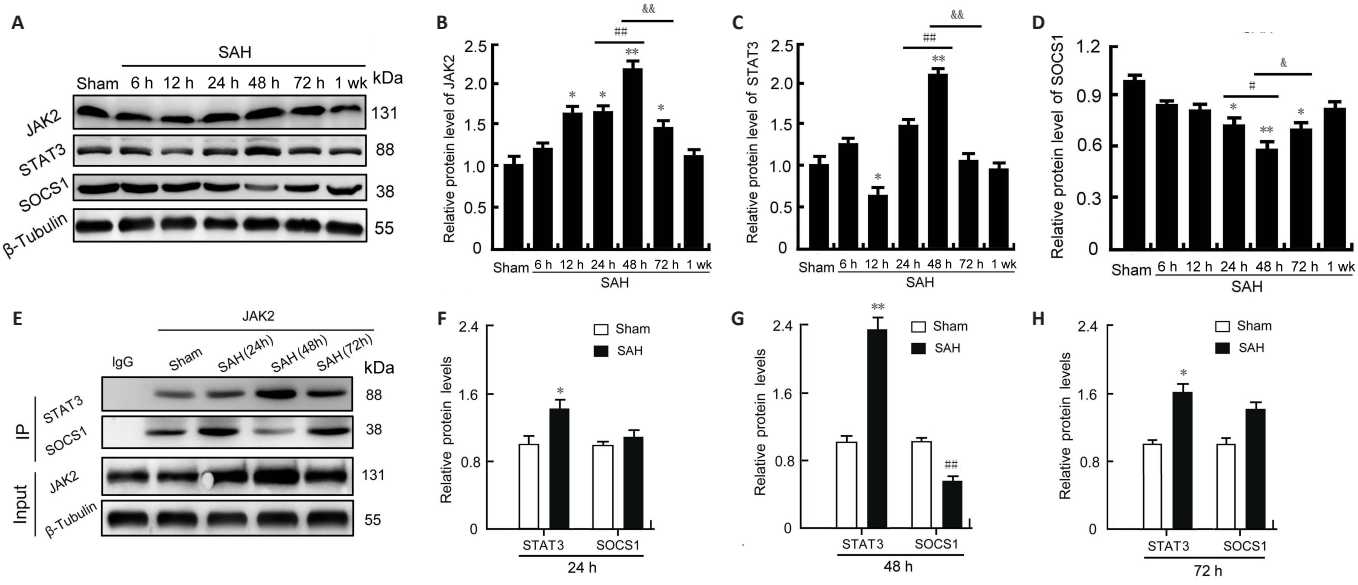

Figure 2 | **Protein expression and interactions of the SOCS1/JAK2/STAT3 axis after SAH.**

(A) Representative bands of JAK2, STAT3, and SOCS1 protein detected by western blot assay. (B–D) Protein expression levels of JAK2, STAT3, and SOCS1. (E) Sample lysates with JAK2 antibody (IgG was used as a negative control); STAT3 and SOCS1 were measured by IP. (F–H) Quantitative analysis of JAK2 and STAT3, and of JAK2 and SOCS1, at 24, 48, and 72 hours following SAH. The Sham group was used as the control. Data are shown as the mean ± SEM ($n = 6$). *$P < 0.05$, **$P < 0.01$, *vs*. Sham group; #$P < 0.05$, ##$P < 0.01$, *vs*. 24-hour SAH groups; &$P < 0.05$, &&$P < 0.01$ *vs*. 72-hour SAH group (one-way analysis of variance followed by Scheffé's *post hoc* test). IP: Immunoprecipitation; JAK2: Janus kinase 2; SAH: subarachnoid hemorrhage; SOCS1: suppressors of cytokine signaling 1; STAT3: signal transducer and activator of transcription 3.

Silencing/overexpressing JAK2 and STAT3 alleviates/aggravates the increased phosphorylation of JAK2 and STAT3 and improves/reduces SOCS1 levels after experimental SAH

Western blot assay was used to assess target protein expression in the brain after treatment with Si-JAK2, Si-STAT3, Over-JAK2, and Over-STAT3 (**Figure 4**). The expression levels of p-JAK2, JAK2, p-STAT3, and STAT3 were significantly higher in the SAH, Si-NC, and Vector groups compared with the Sham group ($P < 0.01$). In contrast, the expression levels of p-JAK2, JAK2, p-STAT3, and STAT3 were significantly lower in the Si-JAK2 and Si-STAT3 groups compared with the Si-NC group ($P < 0.01$ or $P < 0.05$). Over-JAK2 and Over-STAT3 treatments resulted in significantly higher protein levels of p-JAK2, JAK2, p-STAT3, and STAT3 compared with the Vector group ($P < 0.05$). Conversely, both Si-JAK2 and Si-STAT3 treatment improved the reduced SOCS1 expression after SAH ($P < 0.01$), and Over-JAK2 and Over-STAT3 treatment further attenuated SOCS1 expression compared with the Si-NC and Vector groups, respectively ($P < 0.01$). Moreover, immunofluorescent staining showed similar trends in JAK2, STAT3, and SOCS1 expression in neurons after SAH (**Figure 5**).

Silencing JAK2 or STAT3 reduces BBB permeability and brain edema after experimental SAH, whereas overexpressing JAK2 or STAT3 exerts opposite effects

The extent of SAH-induced BBB damage was examined by measuring albumin exudation (**Figure 6A** and **B**). Albumin levels in the SAH group were significantly higher than in the Sham group ($P < 0.01$). Compared with the Si-NC and SAH groups, the albumin levels in the Si-JAK2 and Si-STAT3 groups were significantly lower ($P < 0.01$). Albumin levels in the Over-JAK2 and Over-STAT3 groups were higher than in the Vector group ($P < 0.05$). However, there were no significant differences between the Si-JAK2 and Si-STAT3 groups or the Over-JAK2 and Over-STAT3 groups. We also measured FITC-dextran penetrability (**Figure 6C**), and found that FITC-dextran fluorescence intensity was stronger in the SAH group than in the Sham group ($P < 0.01$). Si-JAK2 and Si-STAT3 treatments alleviated BBB damage ($P < 0.05$), whereas Over-JAK2 and Over-STAT3 aggravated BBB damage ($P < 0.05$). Furthermore, we assessed the degree of SAH-induced cerebral edema (**Figure 6D**). The edema index was higher in the SAH group than in the Sham group ($P < 0.05$). However, the degree of brain edema was markedly lower after Si-JAK2 and Si-STAT3 interventions ($P < 0.05$), and markedly higher after Over-JAK2 and Over-STAT3 interventions ($P < 0.05$). No significant differences were identified in the brain edema index between the Si-JAK2 and Si-STAT3 groups or the Over-JAK2 and Over-STAT3 groups.

Silencing/overexpressing JAK2 or STAT3 decreases/increases SAH-induced cortical cell apoptosis and degradation

To investigate the effects of the SOCS1/JAK2/STAT3 axis on SAH-induced EBI, cortical cell apoptosis and degradation were tested using TUNEL (**Figure 6E** and **F**) and Fluoro-Jade B (**Figure 6G** and **H**) staining. Compared with the Sham group, the proportions of TUNEL- and Fluoro-Jade B-positive cells in brain tissue were significantly higher in the SAH, Si-NC, and Vector groups ($P < 0.01$) and significantly lower in the Si-JAK2 and Si-STAT3 groups ($P < 0.01$). Moreover, the proportions of TUNEL- and Fluoro-Jade B-positive cells were significantly higher in the Over-JAK2 and Over-STAT3 groups compared with the Si-NC, Vector, and SAH groups ($P < 0.01$ or $P < 0.05$).

Silencing JAK2 or STAT3 attenuates M1-type microglial conversion, inhibits pro-inflammatory factors, and augments anti-inflammatory factors

We next investigated the effects of the SOCS1/JAK2/STAT3 axis on microglial phenotypes in the different groups after SAH using immunofluorescence staining (**Figure 7A** and **B**). The results indicated that SAH-induced microglia polarization was mainly of the pro-inflammatory phenotype (CD16-/Iba-1-positive). The ratio of CD16-/Iba-1-positive cells was higher in the SAH, Si-NC, and Vector groups compared with the Sham group ($P < 0.001$). This ratio of CD16-/Iba-1-positive cells was significantly attenuated by Si-JAK2 and Si-SATA3 treatments ($P < 0.001$) and aggravated by Over-JAK2 and Over-STAT3 ($P < 0.01$). The concentrations of pro-inflammatory cytokines (inducible nitric oxide synthase (iNOS), TNF-α, and IL-1β) (**Figure 7C–F**) and anti-inflammatory cytokines (arginase-1, IL-4, IL-10) (**Figure 7G–J**) were measured in the brain tissue of rats using western blot assay. Our experimental results showed that the levels of pro-inflammatory-related molecules increased after SAH, while the levels of anti-inflammatory-related molecules decreased significantly ($P < 0.01$ or $P < 0.05$). Treatment with Si-JAK2 or Si-STAT3 significantly reduced the levels of iNOS, TNF-α, and IL-1β and increased the levels of arginase-1, IL-4, and IL-10 compared with their respective control groups ($P < 0.01$ or $P < 0.05$). In contrast, upregulation of JAK2 and STAT3 (by transfection with Over-JAK2 and Over-STAT3) increased the levels of iNOS, TNF-α, and IL-1β and reduced the levels of arginase-1, IL-4, and IL-10 ($P < 0.01$ or $P < 0.05$).

Silencing/overexpressing JAK2 or STAT3 improves/aggravates neurocognitive function in SAH-induced rats

The effects of modulation of the SOCS1/JAK2/STAT3 axis on rat sensory function were investigated. Both short-term (1–7 days) and long-term (10–35 days) post-SAH, the adhesive-removal test was conducted to evaluate fine sensorimotor function and forelimb coordination (**Figure 8A–D**). Postoperative rats took longer to remove the stickers under the SAH condition ($P < 0.001$). However, when JAK2 and STAT3 were silenced, this duration was significantly shortened ($P < 0.01$ or $P < 0.05$). In contrast, when JAK2 and STAT3 were overexpressed, this duration was significantly lengthened ($P < 0.001$ or $P < 0.01$). Rat locomotor function was also evaluated using the rotarod test (**Figure 8E–H**). Locomotor ability was significantly reduced following SAH ($P < 0.001$), while Si-JAK2 and Si-STAT3 treatments promoted the recovery of function ($P < 0.001$ or $P < 0.01$) and Over-JAK2 and Over-STAT3 delayed the recovery of function ($P < 0.001$). Furthermore, spatial and motor learning abilities following SAH in rats were investigated using the Morris water maze test. Representative trajectories of each group are shown in **Figure 9A–H**. In the Morris water maze test, the escape latency of the SAH group was significantly longer than that of the Sham group ($P < 0.001$; **Figure 9I** and **J**). However, there were no apparent differences among the SAH, Si-NC, and Si-Vector groups. Interestingly, the escape latencies in the Si-JAK2 and Si-STAT3 groups had no short-term differences (**Figure 9K**), but were lower compared with the Si-NC group in the long-term after SAH ($P < 0.001$; **Figure 9L**), whereas the escape latencies of the Over-JAK2 and Over-STAT3 groups had no short-term differences (**Figure 9K**), but were significantly higher compared with the Vector group in the long-term after SAH ($P < 0.001$; **Figure 9L**). In addition, swimming distances in the SAH, Si-NC, and Vector groups were significantly higher compared with the Sham group ($P < 0.001$; **Figure 9M** and **N**). The swimming distances in the Si-JAK2 and Si-STAT3 groups had no short-term differences (**Figure 9O**), but were lower compared with the Si-NC group in the long-term after SAH ($P < 0.001$; **Figure 9P**). Moreover, although the swimming distances of the Over-JAK2 and Over-STAT3 groups also had no short-term differences (**Figure 9O**), they were significantly higher compared with the SAH group in the long-term after SAH ($P < 0.001$; **Figure 8P**). In summary, no significant differences were observed among the SAH, Si-NC, and Si-Vector groups.

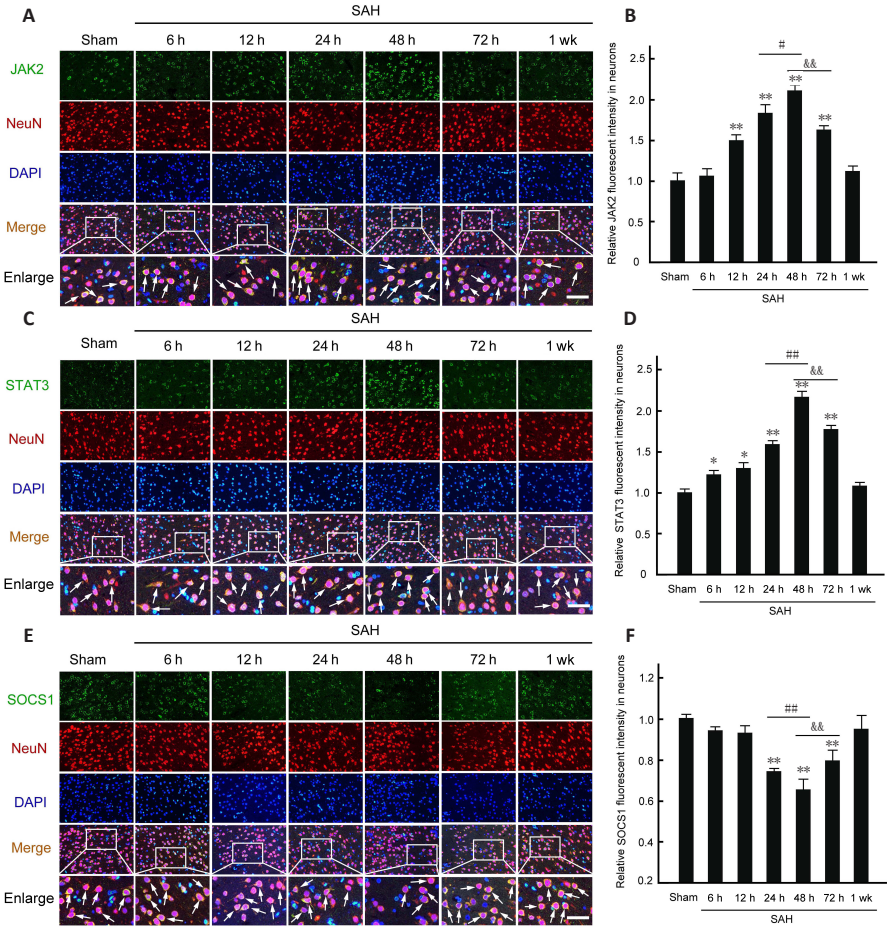

Figure 3 | Immunopositivity of JAK2, STAT3, and SOCS1 in neurons after SAH.
(A, C, E) Double immunofluorescence analysis of JAK2, STAT3, and SOCS1 (green, Alexa Fluor 488) and a neuronal marker (NeuN; red, Alexa Fluor 555) in neurons; nuclei were stained with DAPI (blue). Arrows indicate JAK2-, STAT3-, and SOCS1-immunoreactive neurons. Compared with the Sham group, the immunopositivity of JAK2 and STAT3 was significantly increased at 48 hours after SAH, and the immunopositivity of SOCS1 was significantly decreased. Scale bars: 100 μm. (B, D, F) Immunopositivity of JAK2, STAT3, and SOCS1 in neurons. The Sham group was used as the standard. Data are shown as the mean ± SEM (n = 6). *P < 0.05, **P < 0.01, *vs.* Sham group; #P < 0.05, ##P < 0.01, *vs.* 24-hour SAH group; &&P < 0.01, *vs.* 72-hour SAH group (one-way analysis of variance followed by Scheffé's *post hoc* test). DAPI: 4′,6-Diamidino-2-phenylindole; JAK2: Janus kinase 2; SAH: subarachnoid hemorrhage; SOCS1: suppressors of cytokine signaling 1; STAT3: signal transducer and activator of transcription 3.

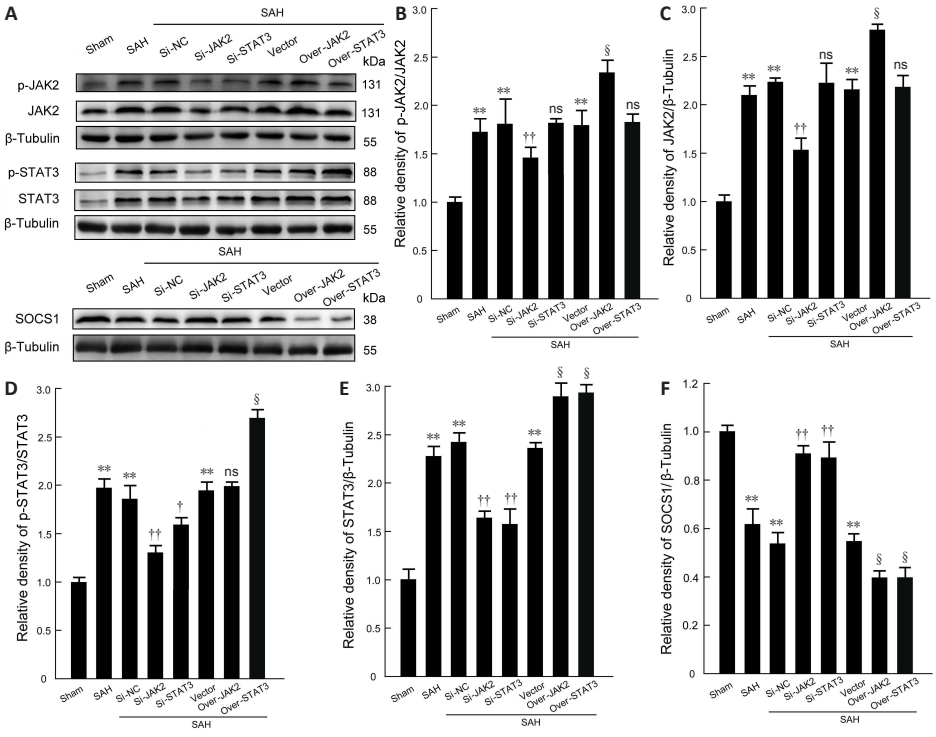

Figure 4 | Effects of silencing/overexpressing JAK2 and STAT3 on the activation of the SOCS1/JAK2/STAT3 axis.
(A) Representative bands of p-JAK2, JAK2, p-STAT3, STAT3, and SOCS1 expression. (B–F) Quantitative analyses of p-JAK2 (B), JAK2 (C), p-STAT3 (D), STAT3 (E), and SOCS1 (F). All data are expressed as the mean ± SEM (n = 6). **P < 0.01, *vs.* Sham group; †P < 0.05, ††P < 0.01, *vs.* Si-NC group; §P < 0.05, *vs.* Vector group. JAK: Janus kinase 2; ns: not significant; SAH: subarachnoid hemorrhage; Si-JAK2: JAK2 small interfering RNA; Si-NC: negative control small interfering RNA; Si-STAT3: STAT3 small interfering RNA; SOCS1: suppressors of cytokine signaling 1; STAT3: signal transducer and activator of transcription 3.

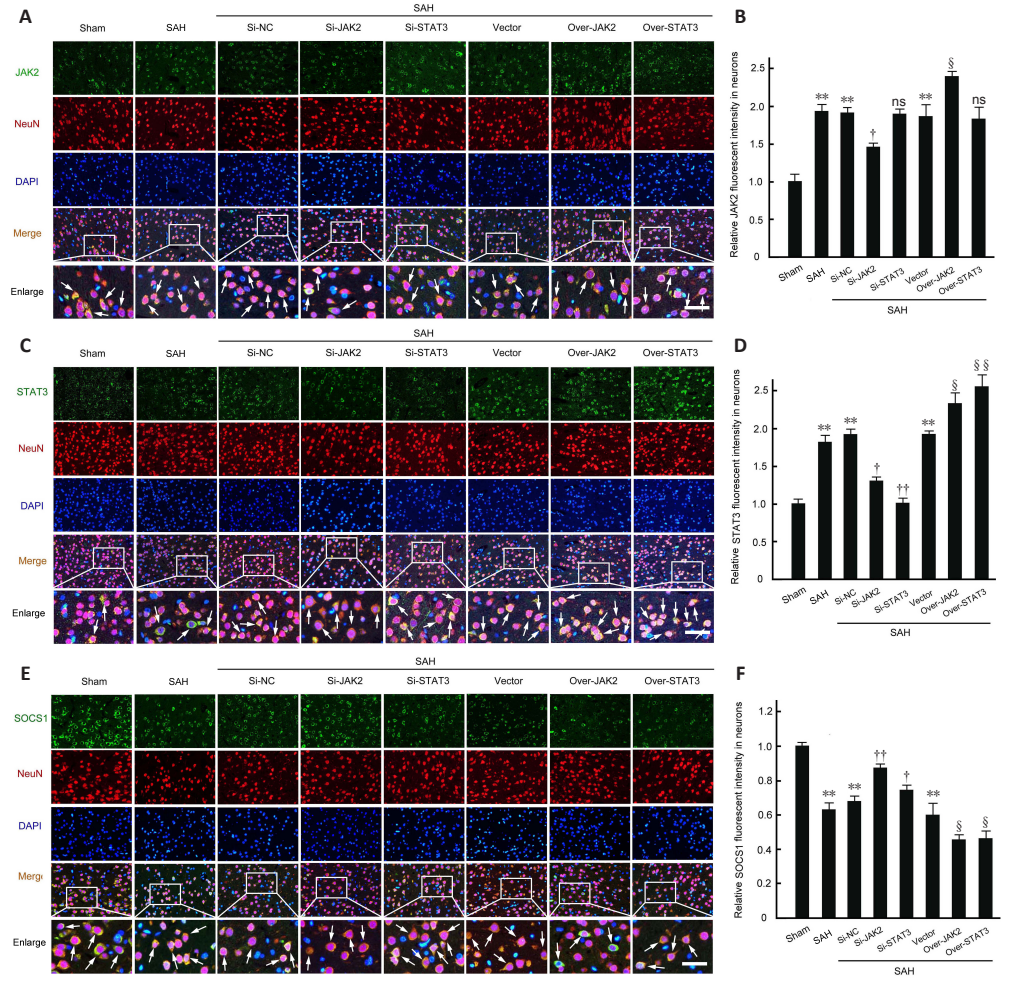

Figure 5 | Immunopositivity of JAK2, STAT3, and SOCS1 in neurons following silencing/overexpressing JAK2 and STAT3 under experimental SAH conditions.

(A, C, E) Double immunofluorescence analysis of antibodies against JAK2, STAT3, and SOCS1 (green, Alexa Fluor 488) and a neuronal marker (NeuN; red, Alexa Fluor 555) in neurons; nuclei were stained with DAPI (blue). Arrows indicate JAK2-, STAT3-, and SOCS1-immunoreactive neurons. Silencing JAK2 and STAT3 decreased the neuronal JAK2 and STAT3 expression and increased the neuronal SOCS1 expression. Conversely, overexpressing JAK2 and STAT3 increased the neuronal JAK2 and STAT3 expression and decreased the neuronal SOCS1 expression. Scale bars: 100 μm. (B, D, F) Immunopositivity of JAK2, STAT3, and SOCS1 in neurons; data are shown as the mean ± SEM (n = 6). $^{**}P < 0.01$, *vs.* Sham group; $^{\dagger}P < 0.05$, $^{\dagger\dagger}P < 0.01$, *vs.* Si-NC group; $^{\S}P < 0.05$, $^{\S\S}P < 0.01$, *vs.* Vector group (one-way analysis of variance followed by Scheffé's *post hoc* test). DAPI: 4′,6-Diamidino-2-phenylindole; JAK2: Janus kinase 2; ns: not significant; SAH: subarachnoid hemorrhage. Si-JAK2: JAK2 small interfering RNA; Si-NC: negative control small interfering RNA; Si-STAT3: STAT3 small interfering RNA; SOCS1: suppressors of cytokine signaling 1; STAT3: signal transducer and activator of transcription 3.

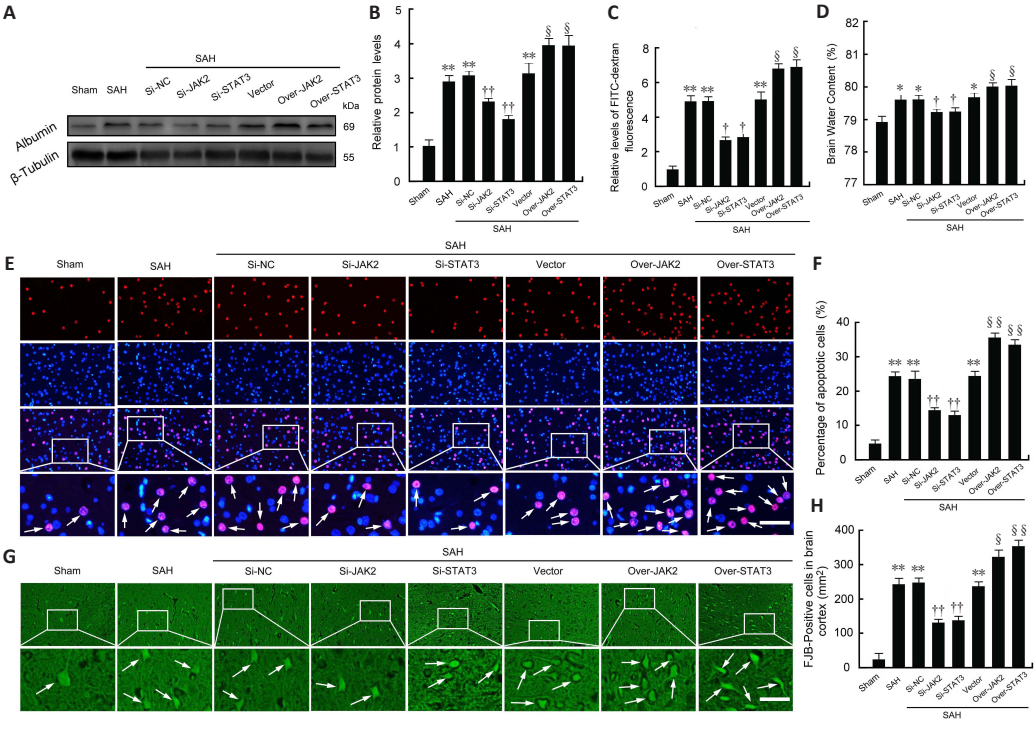

Figure 6 | Effects of silencing/overexpressing JAK2 and STAT3 on blood–brain barrier damage, brain edema, cortical cell apoptosis, and neuronal degeneration after SAH.

(A) Representative bands of albumin detected by western blot assay. (B) Quantitative analysis of albumin protein expression. The Sham group was used as the standard. (C) Relative fluorescein isothiocyanate-dextran fluorescence levels. (D) Brain water content. (E) Apoptotic cells (arrows) in brain tissue. TUNEL-positive cells are red and DAPI is blue. Silencing JAK2 and STAT3 suppressed neuronal cell apoptosis, and overexpressing JAK2 and STAT3 aggravated neuronal cell apoptosis. Scale bars: 100 μm. (F) Quantitative analysis of apoptotic cell percentage. (G) Neuronal degeneration at 48 hours after SAH detected by FJB staining (green). Arrows point to FJB-positive cells. Scale bars: 100 μm. (H) Quantitative analysis of FJB-positive cells. Data are shown as the mean ± SEM (n = 6). $^{*}P < 0.05$, $^{**}P < 0.01$, *vs.* Sham group; $^{\dagger}P < 0.05$, $^{\dagger\dagger}P < 0.01$, *vs.* Si-NC group; $^{\S}P < 0.05$, $^{\S\S}P < 0.01$, *vs.* Vector group (one way analysis of variance followed by Scheffé's *post hoc* test). DAPI: 4′,6-Diamidino-2-phenylindole; JAK: Janus kinase 2; FJB: Fluoro-Jade B; SAH: subarachnoid hemorrhage; Si-JAK2: JAK2 small interfering RNA; Si-NC: negative control small interfering RNA; Si-STAT3: STAT3 small interfering RNA; SOCS1: suppressors of cytokine signaling 1; STAT3: signal transducer and activator of transcription 3; TUNEL: terminal deoxynucleotidyl transferase-mediated dUTP nick end labeling.

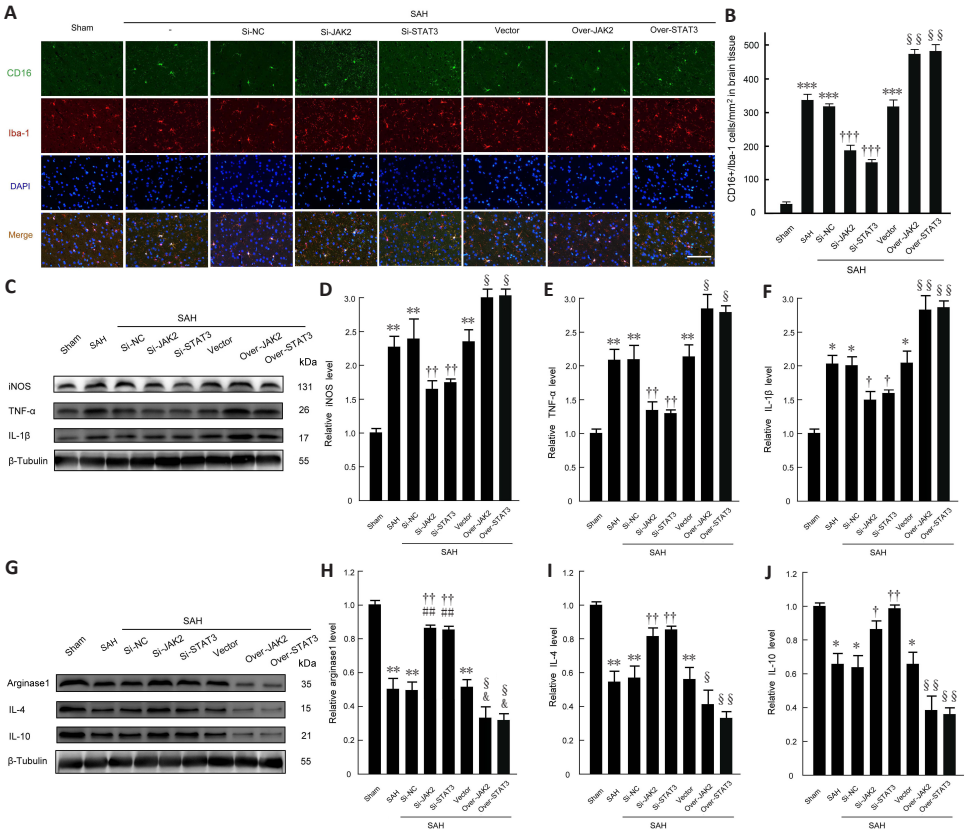

Figure 7 | Effects of silencing/overexpressing JAK2 and STAT3 on microglial conversion into the M1-type phenotype and inflammatory cytokine release after experimental SAH.
(A) Brain sections were stained for CD16 (green; Alexa Fluor 488; M1-type microglia) and Iba-1 (red; Alexa Fluor 555); nuclei were stained with DAPI (blue). Silencing JAK2 and STAT3 suppressed M1-type microglial conversion, and overexpressing JAK2 and STAT3 accelerated M1-type microglial conversion. Arrows indicate M1 microglia. Scale bar: 100 μm. (B) Percentage of CD16-positive cells in all microglia cells. (C, G) Representative bands of iNOS, TNF-α, IL-1β, arginase1, IL-4, and IL-10. (D–F, H–J) Quantitative analyses of iNOS (D), TNF-α (E), IL-1β (F), arginase1 (H), IL-4 (I), and IL-10 (J) expression. The Sham group was used as the standard. Data are shown as the mean ± SEM (n = 6). *P < 0.05, **P < 0.01, ***P < 0.001, *vs.* Sham group; †P < 0.05, ††P < 0.01, †††P < 0.001, *vs.* Si-NC group; §P < 0.05, §§P < 0.01, *vs.* Vector group (one-way analysis of variance followed by Scheffé's *post hoc* test). DAPI: 4′,6-Diamidino-2-phenylindole; Iba-1: ionized calcium-binding adaptor molecule-1; IL: interleukin; iNOS: inducible nitric oxide synthase; JAK2: Janus kinase 2; SAH: subarachnoid hemorrhage; Si-JAK2: JAK2 small interfering RNA; Si-NC: negative control small interfering RNA; Si-STAT3: STAT3 small interfering RNA; SOCS1: suppressors of cytokine signaling 1; STAT3: signal transducer and activator of transcription 3; TNF: tumor necrosis factor.

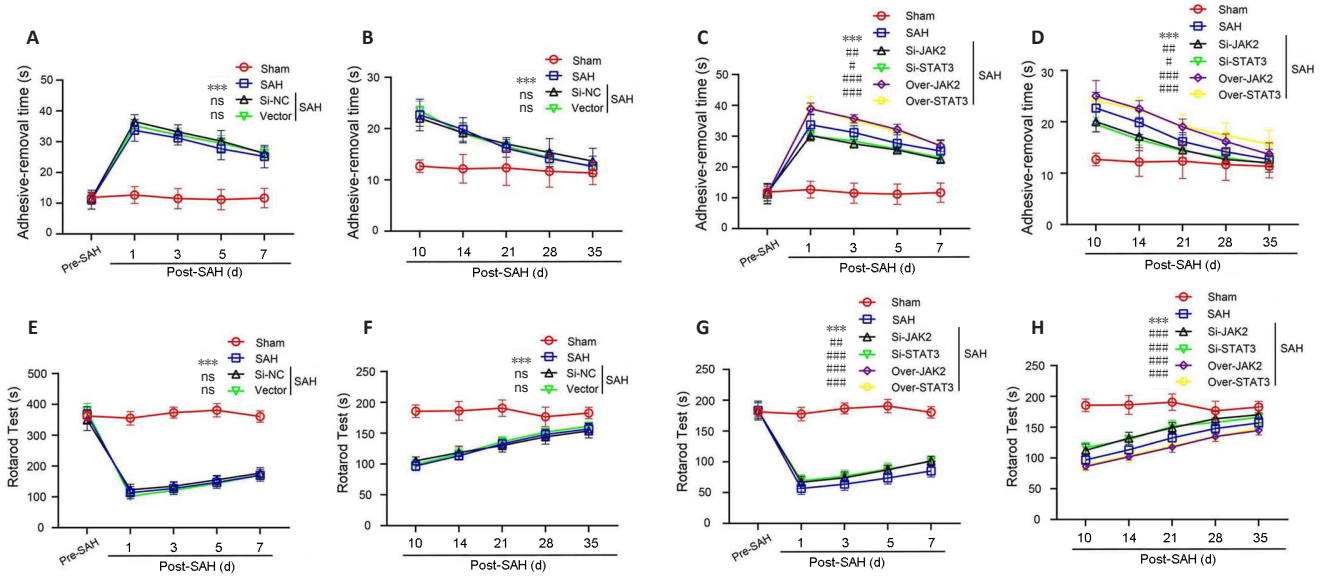

Figure 8 | Effects of silencing/overexpressing JAK2 and STAT3 on the recovery of sensory and locomotor functions in rats after SAH.
(A–D) Adhesive-removal test: Silencing JAK2 and STAT3 accelerated the recovery of sensory function in rats after SAH, and overexpressing JAK2 and STAT3 aggravated the impairment of sensory function. (E–H) Rotarod test: Silencing JAK2 and STAT3 accelerated the recovery of locomotor function in rats after SAH, and overexpressing JAK2 and STAT3 aggravated the impairment of locomotor function. Data are shown as the mean ± SEM (n = 10). ***P < 0.01, *vs*. Sham group; #P < 0.05, ##P < 0.01, ###P < 0.001, *vs*. SAH group (two-way analysis of variance followed by Scheffé's *post hoc* test). JAK2: Janus kinase 2; MWM: Morris water maze; ns: not significant; SAH: subarachnoid hemorrhage; Si-JAK2: JAK2 small interfering RNA; Si-NC: negative control small interfering RNA; Si-STAT3: STAT3 small interfering RNA; SOCS1: suppressors of cytokine signaling 1; STAT3: signal transducer and activator of transcription 3.

AG490 decreases the levels of JAK2 and STAT3 and the interaction between JAK2 and STAT3, but greatly increases the levels of SOCS1 and the interaction between JAK2 and SOCS1 *in vitro* after SAH

To further elucidate the impact of the SOCS1/JAK2/STAT3 axis on neuronal damage, experiments in an *in vitro* SAH model were conducted. Compared with the Control group, immunoprecipitation results showed that neuronal interactions between JAK2 and STAT3 were significantly higher in the OxyHb group, while interactions between JAK2 and SOCS1 were much lower ($P < 0.01$ or $P < 0.05$; **Figure 10A** and **B**). The expression levels of p-JAK2, JAK2, p-STAT3, and STAT3 were significantly higher in the OxyHb group compared with normal neurons, whereas SOCS1 levels were lower ($P < 0.01$). Treatment with AG490 suppressed the expression levels of p-JAK2, JAK2, p-STAT3, and STAT3, and increased SOCS1 expression in OxyHb neurons ($P < 0.01$ or $P < 0.05$; **Figure 10C–H**). Moreover, immunofluorescence staining showed similar trends of JAK2, STAT3, and SOCS1 expression in neurons ($P < 0.001$, $P < 0.01$, or $P < 0.05$; **Figure 10I** and **J**).

Suppression of JAK2 can rescue damaged neurons *in vitro*

The live/dead cellular staining results indicated that the ratio of live/dead neurons in the OxyHb group was lower than that in the Control group ($P < 0.001$). In contrast, there were no differences in survival rates between the OxyHb and Vehicle groups. Nevertheless, neurons treated with AG490 had a much higher survival rate compared with the Vehicle group ($P < 0.01$; **Figure 10K** and **L**).

Discussion

Our results in Experiment 1 demonstrated that the SOCS1/JAK2/STAT3 axis was activated and that JAK2 and STAT3 expression levels were elevated in brain tissue after SAH, whereas SOCS1 expression was reduced. The most noticeable activation time point was 48 hours after SAH. Increased JAK2 and STAT3 and decreased SOCS1 were expressed in neurons. In addition, interactions between JAK2 and SOCS1 decreased after SAH, while interactions between JAK2 and STAT3 were markedly stronger. In Experiments 2 and 3, we found that intracerebroventricular infusions of Si-JAK2 and Si-STAT3 reduced both the phosphorylation levels of JAK2 and STAT3 and the total levels of JAK2 and STAT3, and upregulated SOCS1 levels. In addition, Si-JAK2 and Si-STAT3 treatments attenuated EBI and offered effective neuroprotection by alleviating SAH-induced neuronal apoptosis and degradation, brain edema, BBB injury, and behavioral and cognitive functional impairments. These effects were presumably the result of decreased M1-like phenotype conversion and the inhibition of inflammatory cytokine release after SAH. In contrast, Over-JAK2 and Over-STAT3 interventions exerted an opposite effect, distinctly aggravating EBI after SAH. From these findings, we can conclude that the SOCS1/JAK2/STAT3 axis contributes to EBI by inducing an inflammatory response after SAH. In Experiment 4, we found that AG490 effectively reduced oxyHb-induced neuronal damage by inhibiting the phosphorylation of JAK2 and STAT3 and increasing SOCS1 levels.

Previous studies have indicated that the JAK/STAT signaling pathway is widely involved in inflammatory responses, and that the JAK and STAT kinase families can activate downstream inflammatory signaling pathways (Roxburgh and McMillan, 2016; Morris et al., 2018). As part of the important family of protein tyrosine kinases, there are reports that both JAK2 and STAT3 participate in the downstream events of cytokine receptor binding, such as the transcriptional activation of genes (Chen et al., 2018). Furthermore, JAK and STAT activation processes occur extensively in inflammatory cells in the pancreas and liver (Yu and Kim, 2012). Specifically, cytokines trigger the activation of STAT3, mediated by JAK2. In addition, JAK2 helps to accelerate the activation of STAT3 in the liver. Another study has reported that TNF-α activates JAK2 and STAT3 in the process of pancreatic injury *in vitro*. Inhibiting or blocking the JAK1/STAT1 signaling pathway may reduce its lethal impact on systemic and excessive inflammatory reactions during severe acute pancreatitis (Li et al., 2018b)). Recent research has suggested that thymoquinone treatment reduces the neuroinflammatory response by activating microglia and increasing the expression of these neuroprotective proteins via different signaling pathways (Cobourne-Duval et al., 2018). Nevertheless, the regulatory effects of the SOCS1/JAK2/STAT3 axis on systemic inflammatory responses during SAH, and its association with the degree of brain damage, remain poorly understood because SOCS1 has not been previously investigated in SAH research. We therefore thoroughly studied the possible regulatory effects on pro- and anti-inflammatory cytokines that were mediated by the SOCS1/JAK2/STAT3 axis in the brains of SAH model rats. The protein levels of p-JAK2, JAK2, p-STAT3, and STAT3 increased in the brain, while SOCS1 was markedly decreased both *in vitro* and *in vivo* after SAH. We also demonstrated that the JAK2/STAT3 signaling pathway was rapidly suppressed and SOCS1 levels were improved following AG490 treatment or siRNA intracerebroventricular injection. Moreover, indicators of brain and neuronal damage were improved. It is worth mentioning that SOCS1 plays an inhibitory role in the JAK2/STAT3 signaling pathway. Thus, this finding may indicate that upregulated SOCS1 or suppressed JAK2 and STAT3 levels can reduce inflammatory injury in experimental SAH.

During the inflammatory reaction in the brain, local microglia and macrophages migrate to the injury site and release factors to recruit more immune cells (Zheng et al., 2020). Microglial activation in the brain plays a dual role and can be classified into two phenotypes: a pro-inflammatory phenotype (M1) that destroys neurological function and an anti-inflammatory phenotype (M2) that promotes nerve injury repair. The microglial M1 phenotype can promote the release of cytokines and aggravate the degree of nerve damage. In contrast, M2-type microglia promote the release of neuroprotective factors and help to repair damaged neurons (Yang et al., 2018). Recent studies have reported that M1-type conditioned medium can enhance the death of oligodendrocytes after hypoxia/glucose deprivation *in vitro*, while M2-type conditioned medium has a protective effect. Although many reports have investigated the importance of the M1 and M2 phenotypes in *in vitro* experiments, no consensus has yet been achieved (Meng et al., 2016). In our experiments, the addition of JAK2 and STAT3 inhibitors were able to inhibit the conversion of microglia to the M1 phenotype, thereby reducing neuronal damage. In addition, our results showed that inhibiting the SOCS1/JAK2/STAT3 axis increased the levels of anti-inflammatory factors (IL-4, IL-10, and arginase-1), but reduced pro-inflammatory factor protein levels (iNOS, TNF-α, and IL-1β). This finding further indicates that variations in inflammatory factors may mutually affect M1 and M2 phenotype conversion. Hence, we conclude that the SOCS1/JAK2/STAT3 axis may regulate the SAH-induced inflammatory response from two aspects: microglia conversion and inflammatory factor release.

The present study has several limitations. First, we did not determine the precise mechanism of the SOCS1/JAK2/STAT3 axis in regulating inflammatory factors. In addition, the levels of SOCS1, which is an extremely important factor, were not upregulated or downregulated in our study. Finally, it is difficult to accurately evaluate microglia conversion using immunofluorescence; flow cytometry is a more suitable and accurate method. In conclusion, our study provides adequate evidence to support the potential effects of the SOCS1/JAK2/STAT3 axis and its underlying neuroprotective mechanisms in an experimental SAH rat model. AG490 and Si-JAK2 treatment

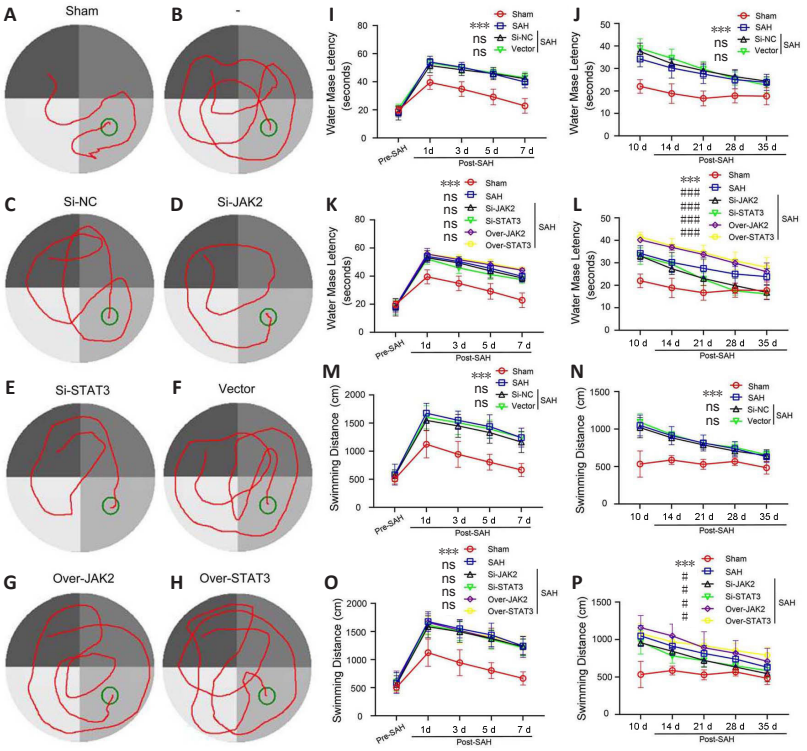

Figure 9 | Effects of silencing/overexpressing JAK2 and STAT3 on the recovery of spatial and motor learning abilities in rats after SAH.

(A–H) Swimming tracks (red) in the MWM. Silencing JAK2 and STAT3 led to a shorter trajectory, and overexpressing JAK2 and STAT3 led to a longer trajectory. The green circle is the target platform. (I–L) Escape latency in the MWM. Silencing JAK2 and STAT3 made the escape latency shorter, and overexpressing JAK2 and STAT3 made the escape latency longer. (M–P) Swimming distance in the MWM. Silencing JAK2 and STAT3 made the swimming distance shorter, and overexpressing JAK2 and STAT3 made the swimming distance longer. Data are shown as the mean ± SEM (n = 10). ***P < 0.01, *vs*. Sham group; #P < 0.05, ###P < 0.001, *vs*. SAH group (two-way analysis of variance followed by Scheffé's *post hoc* test). JAK2: Janus kinase 2; MWM: Morris water maze; ns: not significant; SAH: subarachnoid hemorrhage; Si-JAK2: JAK2 small interfering RNA; Si-NC: negative control small interfering RNA; Si-STAT3: STAT3 small interfering RNA; SOCS1: suppressors of cytokine signaling 1; STAT3: signal transducer and activator of transcription 3.

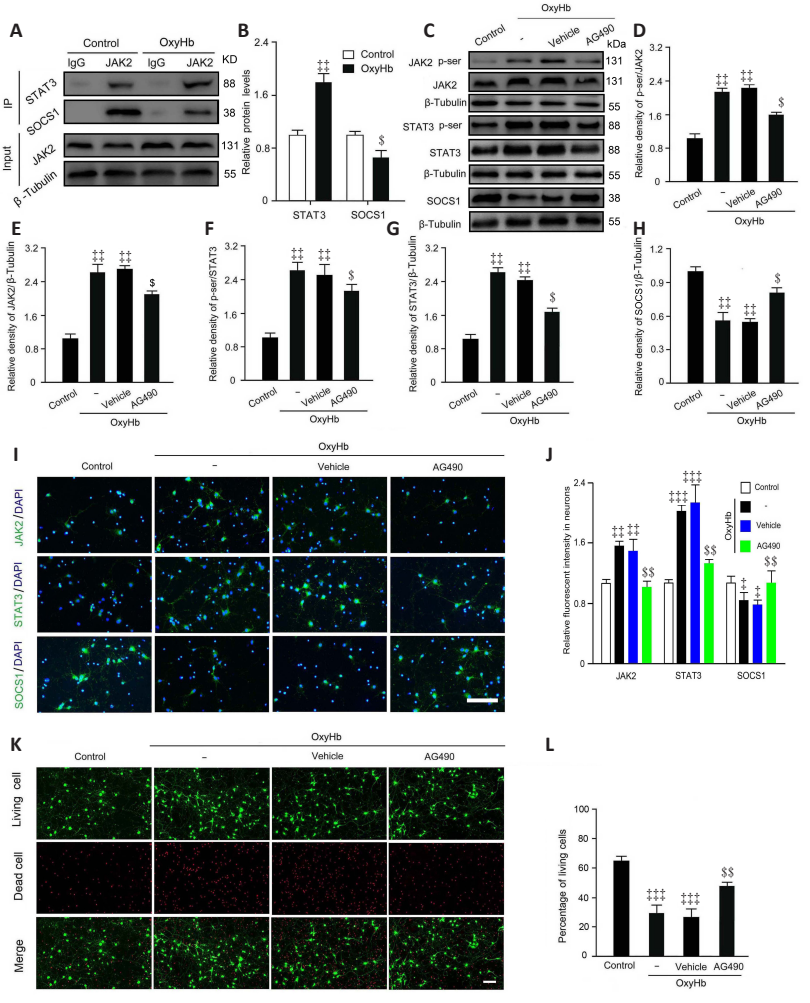

Figure 10 | Effects of AG490 treatment on the interactions and expression of JAK2, STAT3, and SOCS1 in vitro after SAH.

(A) IP of neuronal lysates with JAK2 antibody (IgG was used as a negative control); STAT3 and SOCS1 were detected by immunoblotting. (B) Quantitative analysis of JAK2 and STAT3, and JAK2 and SOCS1. (C) Representative bands of p-JAK2, JAK2, p-STAT3, STAT3, and SOCS1 in cell lysates by western blot assay. (D–H) Quantitative analysis of p-JAK2 (D), JAK2 (E), pSTAT3 (F), STAT3 (G), and SOCS1 (H). (I) Immunofluorescence analysis of JAK2, STAT3, and SOCS1 immunopositivity (green, Alexa Fluor 488); nuclei were stained with DAPI (blue). Arrows indicate JAK2-, STAT3-, and SOCS1-immunoreactive neurons. AG490 suppressed the oxyHb-induced increased expression of JAK2 and STAT3, and improved the oxyHb-induced decreased expression of SOCS1. Scale bars: 32 μm. (J) Quantitative analysis of JAK2, STAT3, and SOCS1 immunopositivity. The control group was used as the standard. (K) Live/dead cellular staining. AG490 improved the survival rates of oxyHb-induced damaged neurons. Green staining represents live neurons and red staining represents dead neurons. Scale bars: 100 μm. (L) Quantitative analysis of live neuron percentages. Data are shown as the mean ± SEM (n = 3). ‡P < 0.05, ‡‡P < 0.01, ‡‡‡P < 0.001, *vs*. control group; $$P$ < 0.05, $$$P$ < 0.01, *vs*. Vehicle group (one-way analysis of variance followed by Scheffé's *post hoc* test). DAPI: 4′,6-Diamidino-2-phenylindole; IP: immunoprecipitation; JAK2: Janus kinase 2; oxyHb: oxyhemoglobin; SAH: subarachnoid hemorrhage; SOCS1: suppressors of cytokine signaling 1; STAT3: signal transducer and activator of transcription 3.

ameliorated the protein expression of key nodes in this axis (specifically, JAK2, STAT3, and SOCS1), and also improved SAH-induced brain edema, cortical neuron apoptosis, and neurological defects. Over-JAK2 and Over-STAT3 treatment had an opposite effect. Moreover, Si-JAK2 and Si-STAT3 treatment inhibited microglial conversion to the M1-type, and also inhibited inflammatory cytokine release. All data in these experiments indicate that the neuroprotective effects of the SOCS1/JAK2/STAT3 axis may result from the inhibition of inflammatory responses after SAH. Therefore, the SOCS1/JAK2/STAT3 axis might function as a therapeutic target in hemorrhagic stroke.

Author contributions: *Study conception and design, quality assurance and control: YFD, CSN; experimental implementation and manuscript writing: YW, XQK; analytic strategy design: FW, BX; literature review, material preparation and method section: DJB, CDC; manuscript reviewing and editing: XPW. All authors approved the final version of the paper.*
Conflicts of interest: *The authors declare that they have no conflict of interest.*
Financial support: *This study was supported by the National Natural Science Foundation of China, No. 81500375 (to XQK); the Fundamental Research Funds for the Central Universities, No. WK9110000112 (to YW); the Anhui Provincial Natural Science Foundation of China, No. 1508085QH184 (to YW); and Shandong Provincial Natural Science Foundation of China, No. ZR2015HQ001 (to XQK). The funding sources had no role in study conception and design, data analysis or interpretation, paper writing or deciding to submit this paper for publication.*
Institutional review board statement: *The study was approved by Animal Ethics Committee of Anhui Medical University and First Affiliated Hospital of University of Science and Technology of China (approval No. LLSC-20180202) on March 1, 2018.*
Copyright license agreement: *The Copyright License Agreement has been signed by all authors before publication.*
Data sharing statement: *Datasets analyzed during the current study are available from the corresponding author on reasonable request.*
Plagiarism check: *Checked twice by iThenticate.*
Peer review: *Externally peer reviewed.*

Open peer reviewers: *Peiman Alesheikh, North Khorasan University of Medical Sciences, Iran; Monireh Azizi, Ilam University of Medical Sciences, Iran.*
Additional file: *Open peer review report 1.*

References

Ahn SH, Savarraj JPJ, Parsha K, Hergenroeder GW, Chang TR, Kim DH, Kitagawa RS, Blackburn SL, Choi HA (2019) Inflammation in delayed ischemia and functional outcomes after subarachnoid hemorrhage. J Neuroinflammation 16:213.
Armstead WM, Hekierski H, Pastor P, Yarovoi S, Higazi AA, Cines DB (2019) Release of IL-6 after stroke contributes to impaired cerebral autoregulation and hippocampal neuronal necrosis through NMDA receptor activation and upregulation of ET-1 and JNK. Transl Stroke Res 10:104-111.
Chen JH, Wu T, Xia WY, Shi ZH, Zhang CL, Chen L, Chen QX, Wang YH (2020) An early neuroprotective effect of atorvastatin against subarachnoid hemorrhage. Neural Regen Res 15:1947-1954.
Chen SP, Sun J, Zhou YQ, Cao F, Braun C, Luo F, Ye DW, Tian YK (2018) Sinomenine attenuates cancer-induced bone pain via suppressing microglial JAK2/STAT3 and neuronal CAMKII/CREB cascades in rat models. Mol Pain 14:1744806918793232.
Cobourne-Duval MK, Taka E, Mendonca P, Soliman KFA (2018) Thymoquinone increases the expression of neuroprotective proteins while decreasing the expression of pro-inflammatory cytokines and the gene expression NFκB pathway signaling targets in LPS/IFNγ-activated BV-2 microglia cells. J Neuroimmunol 320:87-97.
Durham GA, Williams JJL, Nasim MT, Palmer TM (2019) Targeting SOCS proteins to control JAK-STAT signalling in disease. Trends Pharmacol Sci 40:298-308.
Groner B, von Manstein V (2017) Jak Stat signaling and cancer: Opportunities, benefits and side effects of targeted inhibition. Mol Cell Endocrinol 451:1-14.
Hall A, O'Kane R (2018) The extracranial consequences of subarachnoid hemorrhage. World Neurosurg 109:381-392.
Hasegawa S, Hasegawa Y, Miura M (2017) Current therapeutic drugs against cerebral vasospasm after subarachnoid hemorrhage: a comprehensive review of basic and clinical studies. Curr Drug Deliv 14:843-852.
Korja M, Kaprio J (2016) Controversies in epidemiology of intracranial aneurysms and SAH. Nat Rev Neurol 12:50-55.
Li M, Zhang X, Wang B, Xu X, Wu X, Guo M, Wang F (2018a) Effect of JAK2/STAT3 signaling pathway on liver injury associated with severe acute pancreatitis in rats. Exp Ther Med 16:2013-2021.
Li T, Xu W, Gao L, Guan G, Zhang Z, He P, Xu H, Fan L, Yan F, Chen G (2019) Mesencephalic astrocyte-derived neurotrophic factor affords neuroprotection to early brain injury induced by subarachnoid hemorrhage via activating Akt-dependent prosurvival pathway and defending blood-brain barrier integrity. FASEB J 33:1727-1741.
Li X, Li J, Qian J, Zhang D, Shen H, Li X, Li H, Chen G (2018b) Loss of ribosomal RACK1 (receptor for activated protein kinase C 1) induced by phosphorylation at T50 alleviates cerebral ischemia-reperfusion injury in rats. Stroke:Strokeaha118022404.
Lim EJ, Hong DY, Park JH, Joung YH, Darvin P, Kim SY, Na YM, Hwang TS, Ye SK, Moon ES, Cho BW, Do Park K, Lee HK, Park T, Yang YM (2012) Methylsulfonylmethane suppresses breast cancer growth by down-regulating STAT3 and STAT5b pathways. PLoS One 7:e33361.
Liu FY, Cai J, Wang C, Ruan W, Guan GP, Pan HZ, Li JR, Qian C, Chen JS, Wang L, Chen G (2018) Fluoxetine attenuates neuroinflammation in early brain injury after subarachnoid hemorrhage: a possible role for the regulation of TLR4/MyD88/NF-κB signaling pathway. J Neuroinflammation 15:347.
Macdonald RL, Schweizer TA (2017) Spontaneous subarachnoid haemorrhage. Lancet 389:655-666.
Matsumoto J, Dohgu S, Takata F, Machida T, Bölükbaşi Hatip FF, Hatip-Al-Khatib I, Yamauchi A, Kataoka Y (2018) TNF-α-sensitive brain pericytes activate microglia by releasing IL-6 through cooperation between IκB-NFκB and JAK-STAT3 pathways. Brain Res 1692:34-44.
Meng HL, Li XX, Chen YT, Yu LJ, Zhang H, Lao JM, Zhang X, Xu Y (2016) Neuronal soluble fas ligand drives M1-microglia polarization after cerebral ischemia. CNS Neurosci Ther 22:771-781.
Morris R, Kershaw NJ, Babon JJ (2018) The molecular details of cytokine signaling via the JAK/STAT pathway. Protein Sci 27:1984-2009.
Okada T, Suzuki H (2017) Toll-like receptor 4 as a possible therapeutic target for delayed brain injuries after aneurysmal subarachnoid hemorrhage. Neural Regen Res 12:193-196.
Pencik J, Pham HT, Schmoellerl J, Javaheri T, Schlederer M, Culig Z, Merkel O, Moriggl R, Grebien F, Kenner L (2016) JAK-STAT signaling in cancer: From cytokines to non-coding genome. Cytokine 87:26-36.
Qin H, Holdbrooks AT, Liu Y, Reynolds SL, Yanagisawa LL, Benveniste EN (2012) SOCS3 deficiency promotes M1 macrophage polarization and inflammation. J Immunol 189:3439-3448.
Qin JJ, Yan L, Zhang J, Zhang WD (2019) STAT3 as a potential therapeutic target in triple negative breast cancer: a systematic review. J Exp Clin Cancer Res 38:195.
Rosenblat JD, Brietzke E, Mansur RB, Maruschak NA, Lee Y, McIntyre RS (2015) Inflammation as a neurobiological substrate of cognitive impairment in bipolar disorder: evidence, pathophysiology and treatment implications. J Affect Disord 188:149-159.
Roxburgh CS, McMillan DC (2016) Therapeutics targeting innate immune/inflammatory responses through the interleukin-6/JAK/STAT signal transduction pathway in patients with cancer. Transl Res 167:61-66.
Shi A, Dong J, Hilsenbeck S, Bi L, Zhang H, Li Y(2015) The Status of STAT3 and STAT5 in Human Breast Atypical Ductal Hyperplasia. PLoS One 10:e0132214.
Schneider UC, Xu R, Vajkoczy P (2018) Inflammatory events following subarachnoid hemorrhage (SAH). Curr Neuropharmacol 16:1385-1395.
Sturiale CL, Brinjikji W, Murad MH, Lanzino G (2013) Endovascular treatment of intracranial aneurysms in elderly patients: a systematic review and meta-analysis. Stroke 44:1897-1902.
Tong X, Zhang J, Shen M, Zhang J (2020) Silencing of tenascin-C inhibited inflammation and apoptosis via PI3K/Akt/NF-κB signaling pathway in subarachnoid hemorrhage cell model. J Stroke Cerebrovasc Dis 29:104485.
Vadokas G, Koehler S, Weiland J, Lilla N, Stetter C, Westermaier T (2019) Early antiinflammatory therapy attenuates brain damage after sah in rats. Transl Neurosci 10:104-111.
Walker DG, Whetzel AM, Lue LF (2015) Expression of suppressor of cytokine signaling genes in human elderly and Alzheimer's disease brains and human microglia. Neuroscience 302:121-137.
Wang D, Wen X, Zhang X, Hu Y, Li X, Zhu W, Wang T, Yin S (2018) Molecular characterization and expression of suppressor of cytokine signaling (SOCS) 1, 2 and 3 under acute hypoxia and reoxygenation in pufferfish, Takifugu fasciatus. Genes Genomics 40:1225-1235.
Wang Y, Bao DJ, Xu B, Cheng CD, Dong YF, Wei XP, Niu CS (2019) Neuroprotection mediated by the Wnt/Frizzled signaling pathway in early brain injury induced by subarachnoid hemorrhage. Neural Regen Res 14:1013-1024.
Wang Y, Gao A, Xu X, Dang B, You W, Li H, Yu Z, Chen G (2015) The neuroprotection of lysosomotropic agents in experimental subarachnoid hemorrhage probably involving the apoptosis pathway triggering by cathepsins via chelating intralysosomal iron. Mol Neurobiol 52:64-77.
Wang Z, Chen Z, Yang J, Yang Z, Yin J, Zuo G, Duan X, Shen H, Li H, Chen G (2017) Identification of two phosphorylation sites essential for annexin A1 in blood-brain barrier protection after experimental intracerebral hemorrhage in rats. J Cereb Blood Flow Metab 37:2509-2525.
Wu Y, Xu J, Xu J, Zheng W, Chen Q, Jiao D (2018) Study on the mechanism of JAK2/STAT3 signaling pathway-mediated inflammatory reaction after cerebral ischemia. Mol Med Rep 17:5007-5012.
Yang J, Zhao Y, Zhang L, Fan H, Qi C, Zhang K, Liu X, Fei L, Chen S, Wang M, Kuang F, Wang Y, Wu S (2018) RIPK3/MLKL-mediated neuronal necroptosis modulates the M1/M2 polarization of microglia/macrophages in the ischemic cortex. Cereb Cortex 28:2622-2635.
Yu JH, Kim H (2012) Role of janus kinase/signal transducers and activators of transcription in the pathogenesis of pancreatitis and pancreatic cancer. Gut Liver 6:417-422.
Yuan S, Yu Z, Zhang Z, Zhang J, Zhang P, Li X, Li H, Shen H, Chen G (2019) RIP3 participates in early brain injury after experimental subarachnoid hemorrhage in rats by inducing necroptosis. Neurobiol Dis 129:144-158.
Zhang YL, Cai WJ (2020) Blood brain barrier injury in animal models after cerebral ischemia-reperfusion. Zhongguo Zuzhi Gongcheng Yanjiu 16:2848-2850.
Zheng ZV, Lyu H, Lam SYE, Lam PK, Poon WS, Wong GKC (2020) The dynamics of microglial polarization reveal the resident neuroinflammatory responses after subarachnoid hemorrhage. Transl Stroke Res 11:433-449.

P-Reviewers: Alesheikh P, Azizi M; C-Editor: Zhao M; S-Editors: Wang J, Li CH; L-Editors: Gardner B, Robens J, Qiu Y, Song LP; T-Editor: Jia Y